

Supporting information

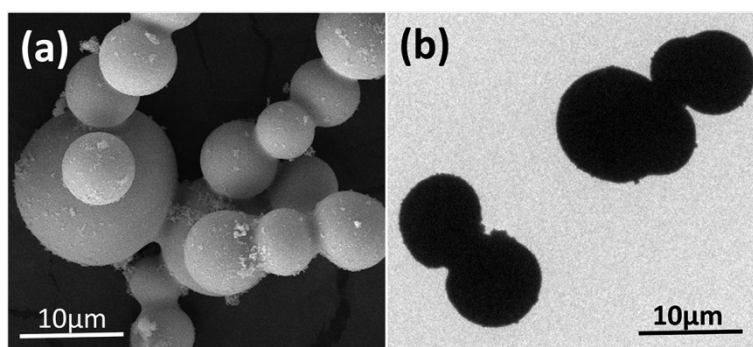


Fig. S1 SEM (a) and (b) TEM images of ZnCo_2O_4 precursors.

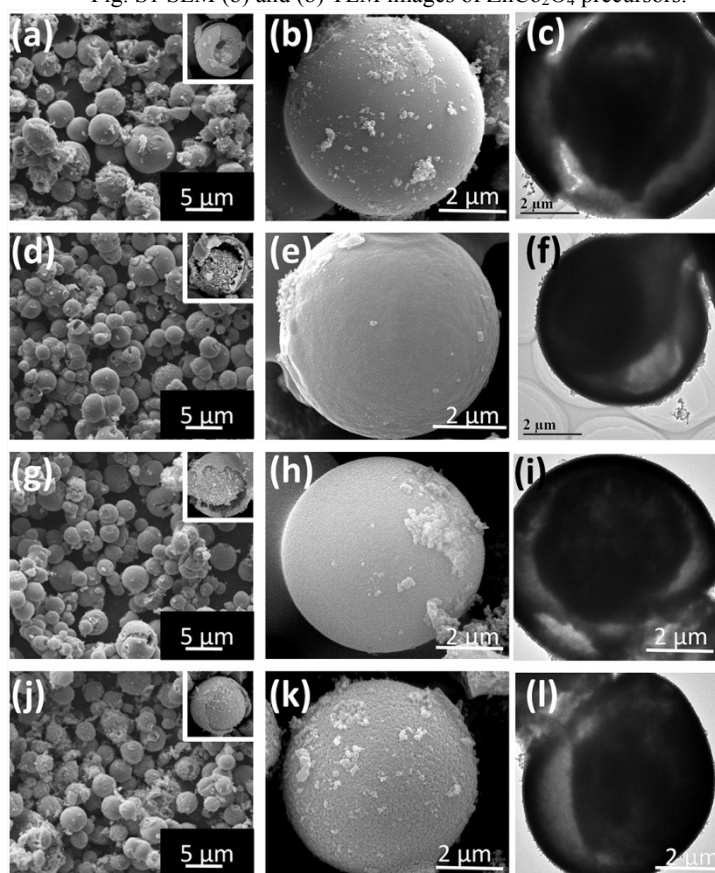


Fig. S2 SEM and TEM images of (a-c) MnCo_2O_4 ; (d-f) NiCo_2O_4 ; (g-i) CoMn_2O_4 ; (j-l) ZnMn_2O_4 microspheres with yolk-shell structure, the insets are corresponding high-magnification SEM images.

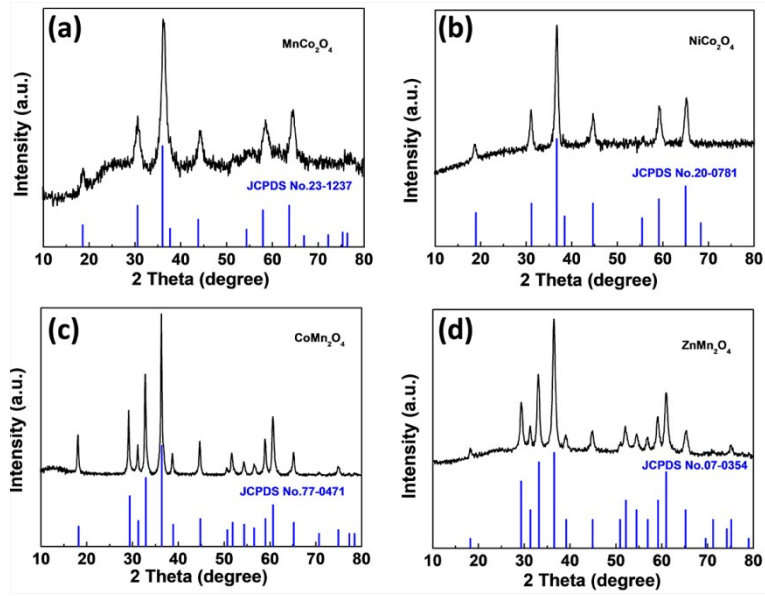


Fig. S3 XRD patterns of (a) MnCo_2O_4 ; (b) NiCo_2O_4 ; (c) CoMn_2O_4 ; (d) ZnMn_2O_4

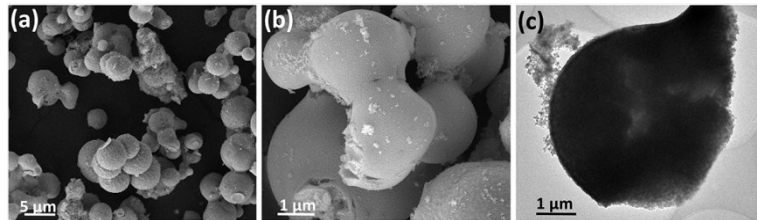


Fig. S4 SEM and TEM images of ZnCo_2O_4 solid microspheres without PEG-400.

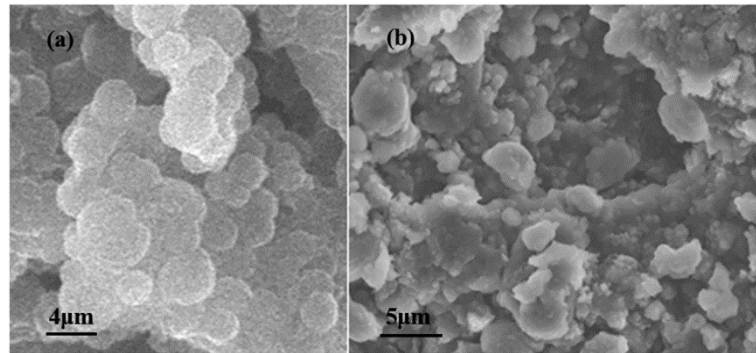


Fig. S5 SEM images of yolk-shell ZnCo_2O_4 microspheres (a) and solid ZnCo_2O_4 microspheres (b) at the current density of 900 mA g^{-1} for 100 cycles.

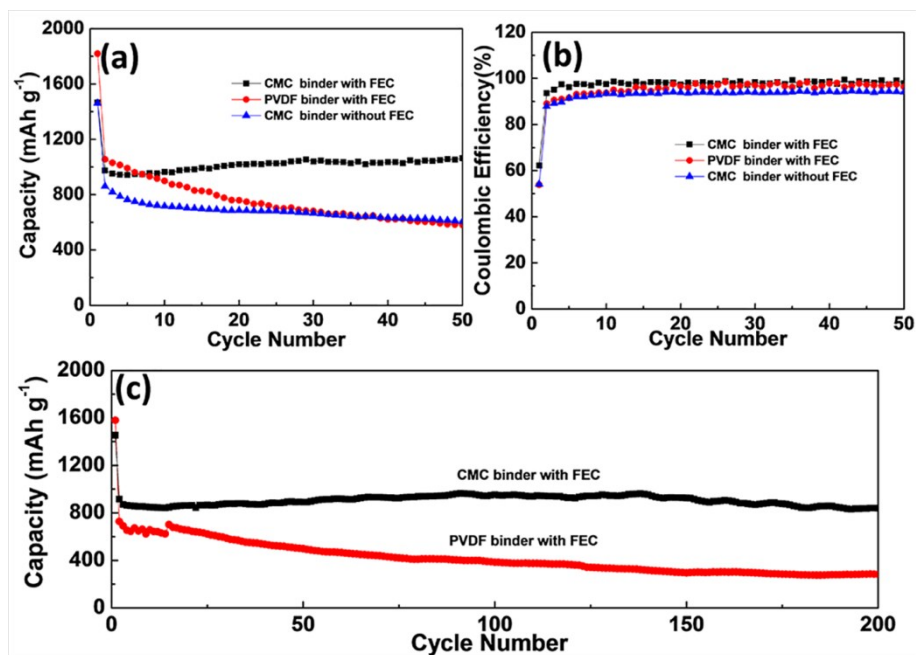


Fig. S6 (a) Cycling performance at the current of $200 \text{ mA} \cdot \text{g}^{-1}$ and (b) coulombic efficiency, (c) discharge cycling performance of ZnCo₂O₄ yolk-shell microspheres at the current density of $900 \text{ mA} \cdot \text{g}^{-1}$ with different binders with or without FEC.